Machine component health prognostics with only truncated histories using geometrical metric approach

Laifa Tao [a,d], Chao Yang [a], Yujie Cheng [a,*], Chen Lu [b,c], Minvydas Ragulskis [e]

[a] School of Aeronautic Science and Engineering, Beihang University, China
[b] School of Reliability and Systems Engineering, Beihang University, China
[c] Science & Technology Laboratory on Reliability & Environmental Engineering, China
[d] Department of Mechanical and Industrial Engineering, University of Toronto, Canada
[e] Research Group for Mathematical and Numerical Analysis of Dynamical Systems, Kaunas University of Technology, Lithuania

ARTICLE INFO

Article history:
Received 30 April 2016
Received in revised form 28 November 2016
Accepted 11 January 2017
Available online 13 March 2017

Keywords:
Time-continuous relevant isometric mapping
Truncated histories
Manifold space
Health prognostics
Survival probability

ABSTRACT

Prognostics plays a vital part in modern decision making for maintenance. Many related valuable approaches have been reported by scientists with both truncated and failure his tories. However, for cases where the actual asserts have no failure histories, one important topic of prognostics is to focus on modeling with only truncated histories. Here we first describe an algorithm called time continuous relevant isometric mapping (TRIM) to estab lish a manifold space where the health state evolutionary laws within truncated histories can be cognized. Unlike classical methods, such as isometric feature mapping, TRIM involves the vital element of state evolution (time), establishes a state evolutionary manifold space by utilizing both local geometrical structures and global isometric features of a given truncated data set. Meantime, two geometrical metrics, neighborhood geodesic distance (NGD) and cumulative geodesic distance, were defined and used in this study to indicate the health state of a given component. Then the feed forward neural network (FFNN) was trained with inputs from the NGD series. The corresponding target vectors (survival probabilities) of FFNN were estimated by intelligent product limit estimator using truncation times and generated failure times. After validation, the FFNN was applied to predict the machine component health of individual component. To validate the proposed method, case study was conducted by using the degradation data generated by a bearing test rig. Results demonstrate that the proposed method can highlight the intrinsic health state evolutionary laws by TRIM even with only truncated histories. The more accuracy prognostics results can be consequently achieved based on the cognition of the evolution ary laws.

1. Introduction

Prognostics is regarded as a kernel and promising tool for realizing condition based maintenance, condition based monitoring, or prognostics and health management [1]. Data driven methods as one important branch of prognostics models have been comprehensively researched. This kind of prognostic models require abundant historical event data, such as continuous observations and failure times.

* Corresponding author.
E-mail address: chengyujie@buaa.edu.cn (Y. Cheng).

In real applications, however, it cannot be acceptable if unexpected failures occur, especially in the cases where the fail ures will result in huge costs and significantly raising safety hazards. To stop these unexpected failures, any unit or compo nent will be replaced or overhauled before it fails once a defect is detected, which makes sense for critical unit or component when no other options are available. Thereby, no further information (e.g. the signals to fail as well as the failure time) related the replaced unit or component will be available for prognostics. The related publications engaging in predicting with these kind of suspended condition monitoring (CM) data sets are limited [2]. Conventional reliability analysis use only failure and suspension times to estimate the lifetime distribution of the probability density function and the cumulative distribu tion function [1,3,4]. In these cases, suspension times are actually treated as failure times and some classical distributions (e.g. Weibull distribution) are widely applied to analyze reliability [5] and to predict residual useful lifetime (RUL).

With the purpose of maximizing the usage of all data available, some models based on degradation data from both failure and suspension histories (including failure and suspension times) were developed. The proportional hazard model estimated the model parameters by incorporating both failure and suspension history data [6]. Moreover, Heng et al. [7] used both the suspended CM and event data in training an intelligent prognostics model, where the survival probability at future time hori zons were achieved [2]. In [8], a two stage statistical method for estimating the fix effect and random effect parameters was developed by using the remaining life distribution model with both failure and suspension histories. In [9], the authors trained a special artificial neural network for predicting the RUL of equipment by utilizing the failure histories and suspen sion histories. In addition, survival analysis and support vector machine were utilized in [10] to establish an intelligent machine prognostics system by utilizing the truncated and un truncated data collected from the CM routine. A residual life prediction model was presented by Gebraeel et al. [11], where the degradation model and prediction process depended both on a degradation database and failure times.

All these preceding methods rely on failure histories. However, as aforementioned, in real world, there are many cases with only truncated histories available (without failure histories), for which these current approaches would not be able to obtain accurate prognostics models. At the same time these cases are also different from those prognostics methods which focus on incomplete data (e.g. sparse, fragmented [12], and partial signals [13,14]).

Recently, a couple of publications attempted to focus on this topic. Zhang et al. [15] developed a method based on neural network with dynamic windows to extrapolate RUL when no failure was available, which showed good performance in case of the stationary indicator rather than non stationary variation degradation indicators. In [16], a functional time warping approach was designed with the assumption that the engineering components degrade according to a common shape func tion with a similar trend. The requirement of either stationary indicator or common shape function widely limits these methods to be applied to the real world.

On the basis of our published paper on the similar topic, we carried out some further researches and developed an algorithm called time continuous relevant isometric mapping (TRIM) to solve these issues. In this study, TRIM, the combi nation of time and geometry, was employed to establish the intrinsic health state manifold where two geometrical metrics, the neighborhood geodesic distance (NGD) and the cumulative geodesic distance (CGD), were defined and were utilized as indicators of machine health. All these preceding developed method and metrics aim to highlight the intrinsic health evolutionary laws under truncated histories. These truncated histories, generated from machine components, generally do not own a stationary indicator or a common shape. In addition, the feed forward neural network (FFNN) was trained by data inputs from the NGD series that correspond to the target vectors of the survival probability, which were estimated by using the intelligent product limit estimator (iPLE) method using the existing truncation times and the generated failure times. After validation, the FFNN was applied to predict the component health of individual units. Case study was conducted by using the degradation data generated by a bearing test rig to validate the proposed method. Results demonstrate that the proposed method can highlight the intrinsic health state evolutionary laws by TRIM. The more accuracy prognostics results can be consequently achieved based on the cognition of the evolutionary laws.

The following sections of this paper are organized to describe clearly the modeling and validation process.

2. Related theories and modified models

2.1. The TRIM algorithm

The isometric feature mapping (ISOMAP) [17] is a global method that maps a dataset from a high dimensional space to a low dimensional space and maintains the global geodesic distances of the corresponding pairwise in the high dimensional space. In this study, the framework of ISOMAP is incorporated into the TRIM algorithm to cognize the health state evolution laws underlying truncated histories.

Originally, the points in the ISOMAP are equally viewed with no differences. Graph G over all data points is constructed by connecting nearby points i and j (closer than a preset e or j is one of the K nearest neighbours of i). The local relationship can be achieved and represented as $d(x_i, x_j)$ with no directivity. K in TRIM is also preset, which denotes the number of the 'nearest time related neighbors' of i. Accordingly, K is no longer obtained by distances but by time related relationships (i.e., each point i has K 'nearest time related neighbors', which are the latest K points ahead of the ith point). The relationship of the ith point and any point j of the latest K ones is denoted as $d_{t\text{-}G}(i, j)$. All the relationships determined within the high dimensional space will be mapped to the low dimensional manifold space (i.e., health state evolutionary manifold space

in this study), where the relationships in the high dimensional space can be well maintained. Moreover, the TRIM algorithm, similar to the ISOMAP algorithm, can be divided into three steps.

(1) Time neighborhood graph (t G) construction

The time graph t G over all data time points is defined by connecting time points i and j if j is one of the latest K time points ahead of the ith time point. The number K can be determined using time series theory. The edge length of time points i and j is $d(x_i, x_j)$.

(2) Computation of shortest time related path for pairwise points

The shortest time related path between the ith time point and any other time point j for arbitrary time point i in a t G is $d_{t\ G}(x_i, x_j)$ $d(x_i, x_j)$ if i, j share one edge (j is one of the latest K points ahead of the ith time point), $d_{t\ G}(x_i, x_j)$ ∞ otherwise. Consequently, $d_{t\ G}(x_i, x_m)$ $\sum_l^i {}_m^1 d_{t\ G}(x_l, x_{l+1})$ for each value of $m = 1, 2, \ldots, i$ K. The final matrix $D_{t\ G}$ $\{d_{t\ G}(x_i, x_j)\}$ will be constructed using the shortest time related path distances between all pairs of time points in G.

(3) d dimensional embedding computation based on the*Multi dimensional Scaling*on distance matrix of [17] $D_{t\ G}$

$$H \equiv \left(I \quad 1_N 1_N^T\right) D_{t\ G} \left(I \quad 1_N 1_N^T\right)/2$$

Let $\lambda_1, \ldots, \lambda_d$ be the top d eigenvalues of H and $\mu_1, \ldots, \mu_d$ be the corresponding eigenvectors. The d dimensional embed dings can then be expressed as T $diag\left(\lambda_1^{1/2}, \ldots, \lambda_d^{1/2}\right) U^T$, where U^T $[\mu_1, \ldots, \mu_d]$.

In this study, TRIM is employed to establish a health state evolutionary manifold (HSEM) where both the truncated CGDs and NGDs can be calculated.

2.2. iPLE calculation

The standard product limit estimator, which computes the survival probability of the total set of samples under study, was modified into iPLE to produce real time survival probability for individual machine component samples [7].

In the case of prognostics with only truncated histories available, we adopted the previous works of Heng et al., who defined the risk of failure in the n next time interval ($risk_{k+n}$) as the conditional probability in which a bearing will fail in time interval $k + n$ given that the bearing has not failed up to time interval k 1. Let F_{k+n} denote the number of failures in time interval $k + n$, and R_{k+n} represent the number of bearings at risk in time interval $k + n$. The risk of a truncated com ponent failing in the k^{th} time interval if left undisturbed is defined as $risk_{k+n} = F_{k+n}/R_{k+n}$.

The standard formula of the Kaplan Meier estimator was modified to produce cumulative survival probability for indi vidual machine component, which is given by

$$S_{k+n} \quad \begin{cases} 1 & 0 \leqslant k+n \leqslant L(i) \\ S_{k+n\ 1}(1 \quad r_{k+n\ 1}) & k+n > L(i) \end{cases}, \tag{1}$$

where k is the "current" time interval, and $L(i)$ denotes the last observed survival time of a machine component. We used the last observed survival time $L(i)$ of each truncated data set as the starting time, rather than time 0, to compute appropriately the survival probabilities of training targets [18].

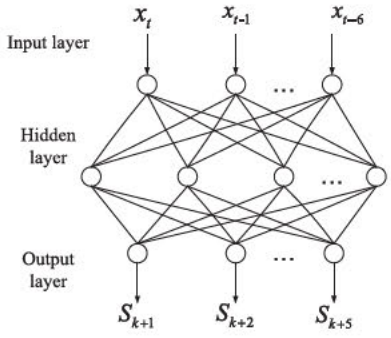

Fig. 1. General structure of the FFNN model.

2.3. FFNN model

Fig. 1 shows the proposed network called feed forward input delay network. In this paper, with the purpose of demonstrating a direct comparison of our work with those carried out in both Refs. [7,19], we set the number of input nodes of FFNN as seven, namely, x_t, x_{t-1}, x_{t-2}, x_{t-3}, x_{t-4}, x_{t-5}, and x_{t-6} (the current component degradation indicator value and six delayed values, which are the inputs from the six previous time steps). A hidden layer made up of 10 hidden nodes was established. The training vector T for each machine component in the training set consists of the survival probability S_{k+n} for each time interval k. For prognostics purposes, five prediction horizons ($n = 1,2,\ldots,5$) were used for the kth time interval with the format $T_k = [S_{k+1}; S_{k+2}; S_{k+3}; S_{k+4}; S_{k+5}]$.

Let k denote the "current" time interval. The first output node represents the survival probability of the machine component at the next time interval (e.g., one time interval = 1 day), S_{k+1}. Let the second output node represent the survival probability of the machine component at the second following time interval (between days 1 and 2, S_{k+2}, and so on, up to the fifth following interval (day 5). Another class was established, that is, the sixth class, which represents the class of components that may survive beyond day 5. The activations of the output nodes were trained with and interpreted as the probability that the machine component would survive up to that time.

3. Health prognostics by utilizing only truncated histories with the combination of TRIM and FFNN

Most of the machine component failure probabilities undergo three typical stages successively, namely, infant mortality, useful life/stable, and wear out [20]. After undergoing the useful life stage during which the state of a machine component is stable and healthy, a machine component begins to deteriorate because of the process of material aging, environment interchange, and so on. In this study, all the truncation times were supposed to be beyond the infant degradation period and contained in the wear out stage. All truncated histories contain degradation information employed to uncover the intrinsic health state evolutionary laws of machines. Unlike the reported machine health prognostics methods, which have both truncated and failure histories to use, we address the challenge of predicting with only truncated histories available by preprocessing, i.e., fitting the CGD series beyond the truncation time for each truncated data set (one truncated data set represents the truncated history of a machine component). On the basis of the assumption mentioned earlier, the key idea is that truncated condition monitoring data contains valuable information reflecting the degradation of equipment, specifically the intrinsic health state evolutionary laws underlying the truncated histories.

Fig. 2 shows the procedure of the proposed geometrical metric based machine component prognostic approach. The details of the approach are presented in the following subsections.

3.1. High dimensional feature extraction

Here we extract features by both time domain and time frequency domain analysis. The final determined eigenvector consists of elements which can reflect some aspects of the evolutionary process, e.g. RMS and energy values. The energy values can be extracted by the wavelet package transformation (WPT) method which is described as follows.

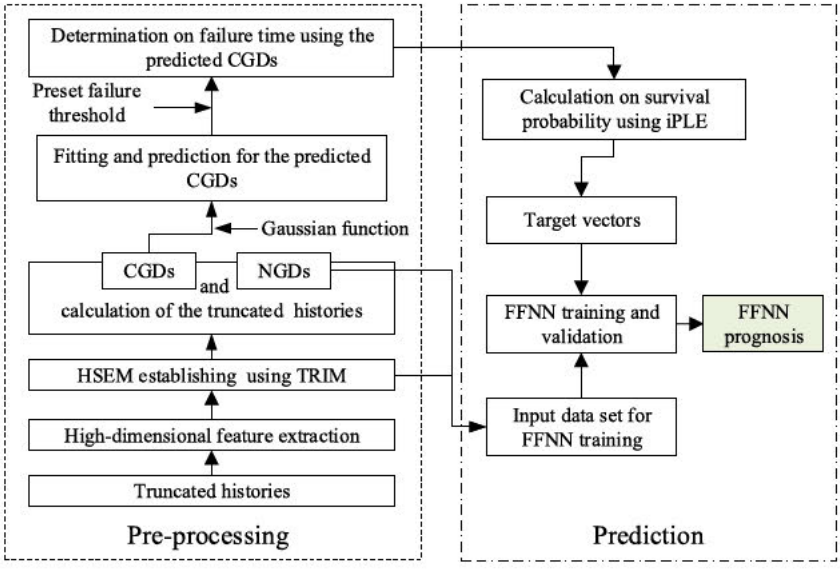

Fig. 2. Procedure of the geometrical approach for machine health prognostics.

Suppose that a segment of a time series, divided from the original vibration signals, is $\{x_k, k \in Z\}$. Through decomposition by using WPT, we obtain the signal X_j, $X_j = \{x_{j,n,l} | j,n,l \in Z\}$, where $x_{j,n,l}$ is the lth sample of the nth packet on the jth level. We define the relative energy for a packet as

$$E(n) \quad \sum_l x_{j,n,l}^2 / \sum_k x_k^2, \tag{2}$$

where $\sum_l x_{j,n,l}^2$ is the energy component of the nth packet on the jth level, and $\sum_k x_k^2$ is the total energy for the segment. Through Eq. (2), the segment is processed to obtain eight relative energies (via WPT at level 3), which will be included in the final high dimensional eigenvector containing nine features in this paper.

3.2. HSEM establishment and the corresponding geometrical metrics

The TRIM algorithm, presented in Section 2.1, is used to map the extracted high dimensional features to a low dimensional HSEM. The inputs of the TRIM algorithm are composed of the high dimensional features extracted from the original machine component signals (i.e., truncated histories). The health degradation state of machine component can then be assessed by the two geometrical metrics, CGD and NGD, which can be calculated based on the established HSEM. The definitions of the two geometrical metrics can be given based on the concept of geodesic distance and can be described as the follow up subsections.

In differential geometry, a geodesic is a generalization of the notion of a straight line to curved spaces. The geodesics are (locally) the shortest path between points in the space (http://en.wikipedia.org/wiki/Geodesic) if this connection is the Levi Civita connection induced by a Riemannian metric. Furthermore, the geodesic distance of two points is the shortest path between the two points lying on a geodesic in the space.

CGD: The geodesic line and the geodesic distance between two arbitrary time points on *HSEM* reflect the similarity or the difference of states at the two time points. The CGD represents the geodesic distance between an arbitrary time point and the origin on *HSEM*, which is a metric of state departure from the origin on *HSEM*.

NGD: The NGD describes the distance between an arbitrary time point and any neighbours of the time point, where the neighbours are defined or calculated when a special number of neighbours or a special radius of a neighborhood is given. Therefore, the NGD is a distance metric between any two arbitrary points on *HSEM* used to depict the local geometrical structure of *HSEM*. In this paper, the number of the neighbours of any given time point was fixed as one to search for the most similar state of the time point.

3.3. Calculation on the truncated CGD and NGD histories

The approximation method employed to calculate the NGDs and CGDs in this study is the method based on graph theory proposed by Tenenbaum et al. in Science 2000.

In this study, TRIM maintains intrinsic geodesic relationship (distances) between time points. Thus, the CGD and NGD obtained from the constructed HSEM indicate the health status of the corresponding time points. Therefore, CGD and NGD are regarded as the geometrical degradation metric of machine component health in this study. The performance degradation trend can be visualized by using the CGD and NGD trend. In this study, CGD series were used to determine the failure times of the selected truncated data sets by Gaussian function and NGD series were formed to act as the inputs of FFNN.

Suppose that for each truncated data set consisting of a series of bearing vibration data segments (e.g. 1024 continuous data points for each segment), we obtain one high dimensional eigenvector from one data segment by high dimensional feature extraction. Thus, for a truncated data set with M segments will have a feature matrix of $M \times N$, where N is the dimension of the high eigenvector. The corresponding CGDs and NGDs on the HSEM constructed by TRIM with the input of $M \times N$ matrix can be calculated.

Let $NGD_{f,k}$ be the NGD value of the kth segment of the fth truncated data set (e.g. the kth NGD value of the vibration data set from the fth bearing).

Thus, the total number of truncated NGD histories is

$$N_{ngd,tru} \quad \sum_{f\ 1}^{F} NQ_f, \tag{3}$$

where NQ_f is the number of NGDs calculated from the HSEM of the truncated data set f, and F represents the number of truncated data sets (e.g. the number of bearings). Similarly, the total number of truncated CGD histories can be noted as $N_{cgd,tru}$, which is equal to $N_{ngd,tru}$.

Furthermore, the total number of input/output pairs for FFNN on the basis of the truncated NGD histories is

$$N_{ngd,tru,ffnn} \quad \sum_{f\ 1}^{F} (NQ_f \quad N_{node,ffnn} + 1), \tag{4}$$

where $N_{node,ffnn}$ denotes the number of input nodes of FFNN.

3.4. Fitting and prediction for the predicted CGDs using Gaussian function

As discussed earlier, after calculating the truncated CGDs based on the truncated histories, curves of the truncated CGDs can be obtained. For each curve i of the truncated CGDs, a Gaussian function is employed to fit and predict the subsequent CGDs which are also the predicted CGDs.

Thus, the failure time of each truncated data set can be determined based both on the predicted CGDs and on a preset failure threshold. All the determined failure times will be used directly to calculate on survival probabilities using iPLE.

3.5. Machine component health prognostics based on FFNN

As described in Section 2.3, the FFNN has seven input nodes (i.e., $N_{node.ffnn}$ 1), which consist of the truncated NGD his tories derived from the original truncated histories based on TRIM. After obtaining the failure time needed for each specified truncated data set by fitting and predicting the truncated CGD series, the survival probability estimations S_k can be derived by using the iPLE method, which is briefly described in Section 2.2. Each target/output vector of FFNN is formatted as

$$T_k \quad [S_{k+1}; S_{k+2}; S_{k+3}; S_{k+4}; S_{k+5}], \tag{5}$$

where S_{k+n} has the form of Eq. (5).

Once trained and validated, the FFNN can be used for the prognostics of individual machine component health. The FFNN outputs that represent the survival probabilities of the machinery in the following five time intervals can be obtained.

When new condition monitoring data are available, all the prognostics process will be performed again and the survival probabilities will be updated. The machine component health prognostics process stops when the equipment fails or when the equipment is preventively taken out of service.

4. Case study

4.1. Dataset description and the criteria of accuracy

In this study, the experimental data was generated from a bearing test rig that can produce run to failure data. These data were downloaded from Prognostics Center of Excellence (PCoE) through prognostic data repository contributed by Intelli gent Maintenance System (IMS), University of Cincinnati (Lee, Qiu, Yu, Lin & Rexnord Technical Services, 2007). The bearing test rig and data acquisition were described in [10]. On the basis of these bearing failure histories, 40 failure history data sets (bearing degradation vibration data), including failure times, were used for the training and testing of the proposed approach.

We employed 30 truncated data sets (truncated from the corresponding actual failure history data sets). 20 of them were selected and seen as failure history data sets by fitting and predicting. 10 of them were treated as truncated data sets. All of these data sets were employed to train the proposed approach. The remaining 10 of the 40 failure history data sets were applied for testing.

Each failure history data set consists of a series of segments (time steps, t). One segment was acquired every 2.4 h, with the length of 20,480 sampling data points in one second. In the test, 10 time steps were grouped as one time interval (i.e. 1 day). The prediction horizon had 5 time intervals (n = 1, 2, 3, 4, 5).

In this case, we calculated the accuracy of every prediction process output. The prediction accuracy can be calculated by Eq. (6), where K_P is the predicted failure time interval, and K_A is the actual failure time interval.

$$Accuracy \quad \left(1 \quad \frac{|KP \quad KA|}{KA}\right) \times 100\%. \tag{6}$$

The failure threshold predetermined in this study was 0.5; i.e., once the survival probability drops below 0.5, the failure time interval is reached. Herein, the failure time interval is representative of the remaining life of bearings.

In this manner, we anticipated several conclusions derived from the proposed and existing methods to validate the effi ciency of the proposed method on predicting with only truncated histories available.

4.2. Pre processing of the proposed approach

A total of 20 data sets, with light blue background in Table 1, were randomly selected from the former 30 truncated data sets of all the 40 data sets and assigned for training to be preprocessed by the TRIM and Gaussian function.

4.2.1. High dimensional feature extraction

As described in Section 3.1, we analyzed the features of these data sets. Figs. 3 and 4 display the 4 features in time domain and 8 features obtained by WPT, respectively. As we can see from the two figures, the states of the bearing kept healthy for a long stable time period and then experienced a sharp drop. This general evolutionary law of health state can be depicted by RMS and other eight energy features, which formed the final high dimensional eigenvector with nine elements in this case.

Table 1
Training data sets for the proposed prognostics mode.

Data set	1	2	3	4	5	6	7	8	9	10	11	12	13	14	15
Actual failure time interval	37	21	11	24	15	16	47	18	34	21	14	28	29	34	14
Truncation time interval	35	21	10	23	13	14	42	16	33	19	13	27	28	33	13
Failure time step	362	–	107	–	146	153	467	170	–	205	130	–	280	336	134
Data set	16	17	18	19	20	21	22	23	24	25	26	27	28	29	30
Actual failure time interval	10	37	27	43	27	29	30	25	22	13	36	18	25	15	24
Truncation time interval	9	35	25	41	25	28	29	24	21	13	34	17	24	14	23
Failure time step	94	–	265	–	261	–	291	249	–	128	–	177	241	–	233

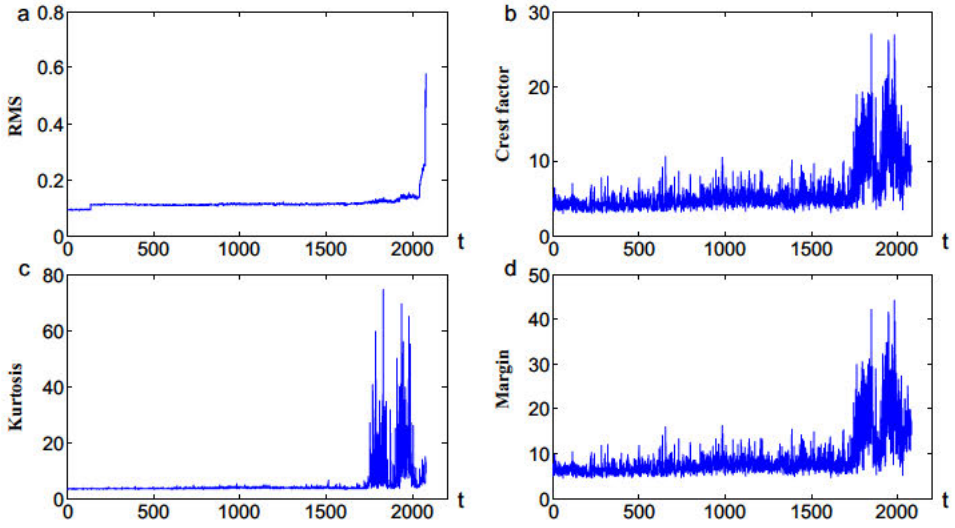

Fig. 3. Feature analysis of the time domain for the vibration data of bearing.

4.2.2. Truncated CGD series and NGD series

Fig. 2 shows that to transform the original truncated histories into truncated CGD series and NGD series, some steps such as high dimensional feature extraction and HSEM establishing based on TRIM should be executed successively. All these steps have been described in the aforementioned sections. A schematic diagram for depicting the NGD series was given in Fig. 5a, in which the stable and infant degradation stages were demonstrated before the truncation time. Meanwhile, a schematic diagram of the CGD series was also plotted in Fig. 5b.

4.2.3. CGD series fitting and prediction based on Gaussian function

To capture the intrinsic health state evolutionary laws in the original truncated histories and the truncated CGD series. In this section, we obtained 20 subsequences of the 20 truncated CGDs by fitting and prediction based on Gaussian function, as shown in Fig. 6. The Gaussian function with the corresponding determined coefficients as well as the accuracy of fitting and prediction were listed in Fig. 7.

As we can see from Figs. 6 and 7, Gaussian function can well recognize the intrinsic laws within the CGD curves which denote the intrinsic health state evolution. The high accuracy of fitting and cognition guarantees a strong support for failure time prediction and further calculation.

As shown in Fig. 6a, the failure time of this truncated data set will be ascertained according to the pre determined failure threshold CGD = 7100 (see also Fig. 5b). Similarly, in this section, we obtained all the failure times of the selected 20 trun cated data sets based on the Gaussian function and the pre determined failure threshold, as listed in Table 1.

4.3. Prognostics by only utilizing truncated histories

4.3.1. Survival probabilities calculation for FFNN

Table 1 shows the data sets in which the selected history data sets and their failure times are highlighted. When 20 failure times of the 20 truncated data sets selected from the specified 30 data sets are determined, then the survival probabilities can be calculated in accordance to the description in Section 2.2.

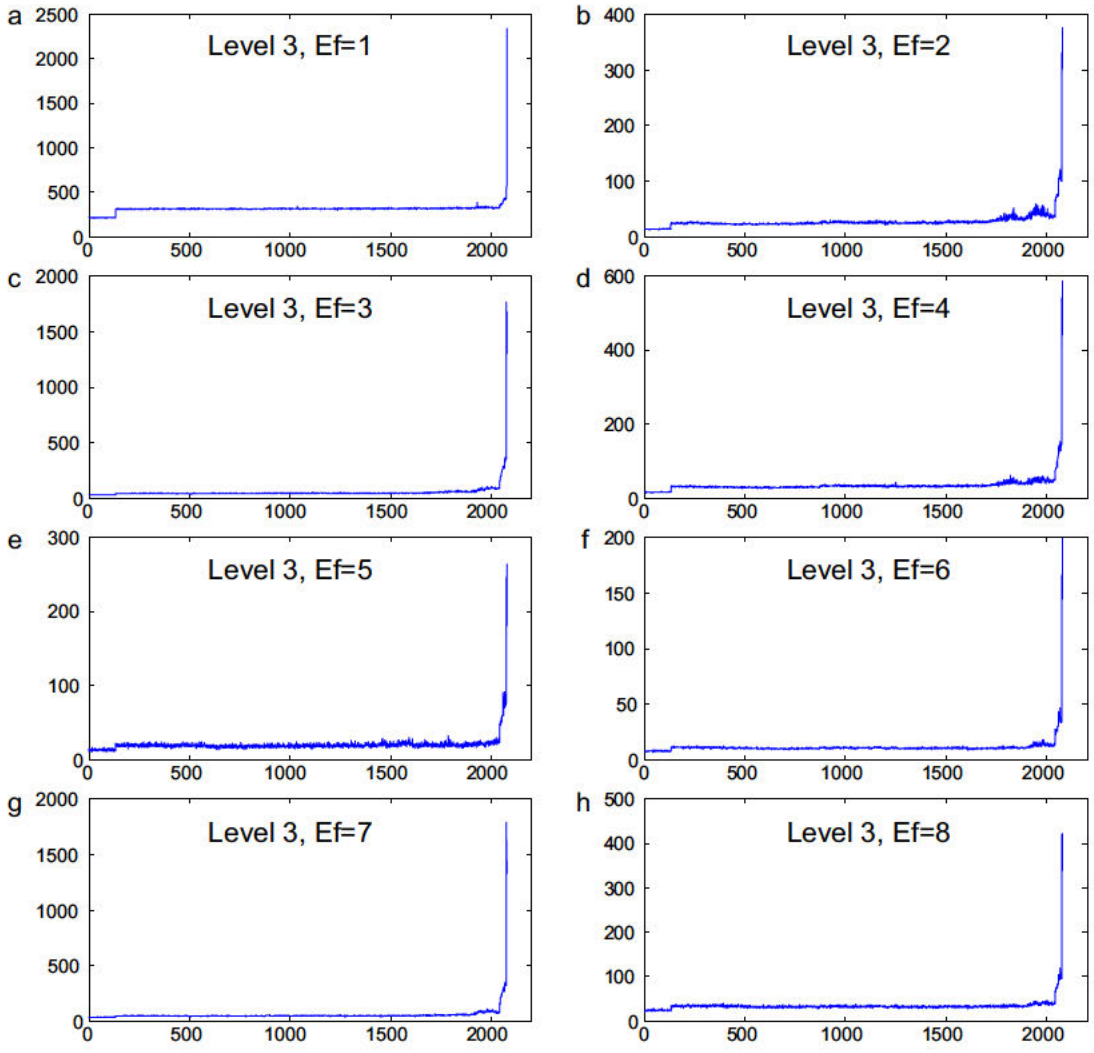

Fig. 4. Feature analysis by WPT based on the vibration data of bearing.

4.3.2. FFNN prognostics

The numbers of the FFNN input, hidden, and output nodes were respectively determined as 7, 10, and 5 [7], in which each of them agrees with the form mentioned in Section 2.3.

The FFNN was trained and validated by the training and testing data sets constructed from the 30 data sets, which consisted of 10 truncated data sets and 20 data sets with the corresponding determined failure times. As shown in Tables 2 and 3, general cases of input (Table 2) and output (Table 3) matrixes of the FFNN are given.

In this section, the 31st data set and its survival probabilities were considered to interpret the prediction process of FFNN.

As shown in Table 4, the values with colored background were the first values that drop below 0.5 (failure threshold) in each columns (e.g. the prediction outputs of the values 0.3594 and 0.2247 at time steps $t = 273$ and $t = 280$, respectively). The failure time interval can be given by the formula:

$$P_k \quad k + \sum_{i\ 1}^{5} n_{(k+i)} \cdot i / \sum_{i} n_{(k+i)}, \tag{7}$$

where k is the time interval, $n_{(k+i)}$ represents the number of values which lie at the prediction horizon of $k+i$ and are with colored background. As the values listed in Table 4, we calculated the lifetime of the 31st bearing with the usage of Eq. (7), the predicted lifetime of the 31st bearing was determined to be 29.25 days, i.e. the 31st bearing would fail in the 30th time interval. Table 5 shows all the prediction results of the survival probabilities as well as the predicted failure time intervals for the 10 testing data sets. Most of the prediction accuracies are greater than 95%, except for the 35th with accuracy of 93.75%.

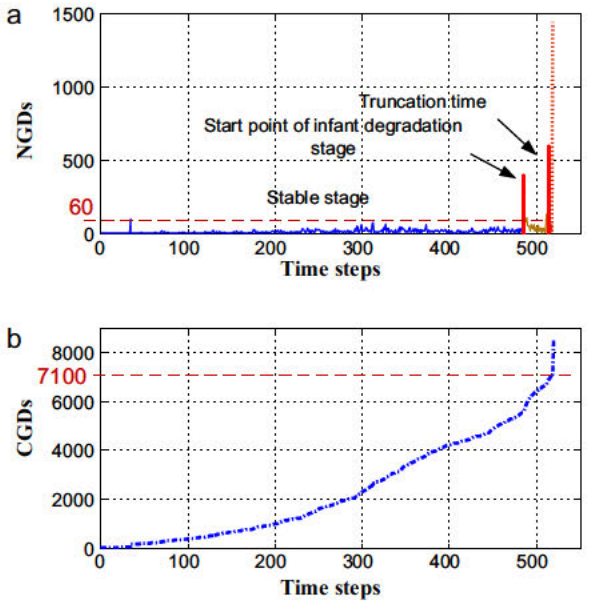

Fig. 5. Life span of a bearing represented by both NGDs and CGDs.

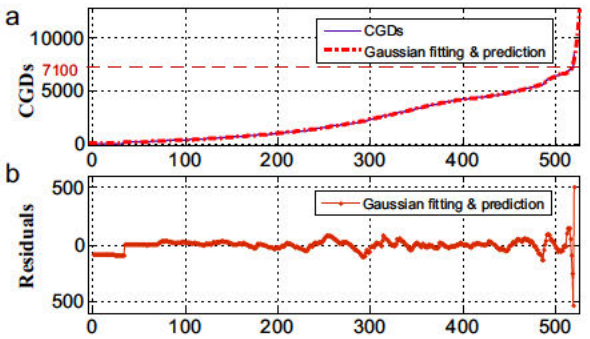

Fig. 6. Fitting and prediction of the CGD sequence by Gaussian function.

General model Gauss6:

f(x) =

a1*exp(-((x-b1)/c1)^2) + a2*exp(-((x-b2)/c2)^2) +
a3*exp(-((x-b3)/c3)^2) + a4*exp(-((x-b4)/c4)^2) +
a5*exp(-((x-b5)/c5)^2) + a6*exp(-((x-b6)/c6)^2)

Coefficients (with 95% confidence bounds):

a1 = -3.72e5 (-1.46e7, 1.38e7)	b1 = 566.5 (186.5, 946.5)	c1 = 30.49 (-81.69, 142.7)
a2 = 1.67e9 (-3.8e11, 3.83e11)	b2 = 723.6 (-3941, 5388)	c2 = 62.36 (-651.2, 775.9)
a3 = -347.6 (-706.7, 11.47)	b3 = 287 (259.8, 314.1)	c3 = 94.16 (57.29, 131)
a4 = -266.5 (-512.1, -20.89)	b4 = 427.1 (412.6, 441.7)	c4 = 32.97 (14.97, 50.96)
a5 = 30.92 (-34.55, 96.39)	b5 = 404.2 (393.1, 415.4)	c5 = 9.422 (-12.09, 30.94)
a6 = 5297 (4348, 6246)	b6 = 505.6 (432.1, 579.1)	c6 = 247.2 (212.9, 281.5)

Goodness of fit:

SSE	R-square	Adjusted R-square	RMSE
1.424e+006	0.9993	0.9993	53.25

Fig. 7. Coefficients and accuracy of the fitting and prediction process by Guaussian function.

Table 2
General cases of the input matrix of FFNN.

No.	1	2	3	4	5	6	7	...
$x(t)$	0.014953	0.030755	0.026762	0.016891	0.0254	0.035078	0.033801	...
$x(t-1)$	0.030755	0.026762	0.016891	0.0254	0.035078	0.033801	0.033859	...
$x(t-2)$	0.026762	0.016891	0.0254	0.035078	0.033801	0.033859	0.029669	...
$x(t-3)$	0.016891	0.0254	0.035078	0.033801	0.033859	0.029669	0.0304	...
$x(t-4)$	0.0254	0.035078	0.033801	0.033859	0.029669	0.0304	0.026258	...
$x(t-5)$	0.035078	0.033801	0.033859	0.029669	0.0304	0.026258	0.018183	...
$x(t-6)$	0.033801	0.033859	0.029669	0.0304	0.026258	0.018183	0.028737	...

Table 3
General cases of the output matrix of FFNN.

Failure cases (the kth time interval)										
$S(k+1)$	1	...	1	1	1	...	1	1	1	...
$S(k+2)$	1	...	1	1	1	...	1	1	0	...
$S(k+3)$	1	...	1	1	1	...	0	0	0	...
$S(k+4)$	1	...	1	0	0	...	0	0	0	...
$S(k+5)$	1	...	0	0	0	...	0	0	0	...
Truncated cases (the kth time interval)										
$S(k+1)$	1	...	1	...	1	...	1	...	0.9000	...
$S(k+2)$	1	...	1	...	1	...	0.9000	...	0.8000	...
$S(k+3)$	1	...	1	...	0.9000	...	0.8000	...	0.6000	...
$S(k+4)$	1	...	0.9000	...	0.8000	...	0.6000	...	0.5000	...
$S(k+5)$	0.9000	...	0.8000	...	0.6000	...	0.5000	...	0.4000	...

Table 4
Prediction results of the 31st bearing.

Horizons	$t=271$	$t=272$	$t=273$	$t=274$	$t=275$	$t=276$	$t=277$	$t=278$	$t=279$	$t=280$
Time interval k	*27*									
$k+1$	0.9871	0.9855	0.8718	0.5012	0.4790	0.7131	0.6284	0.6913	0.6580	0.2247
$k+2$	0.9635	0.9590	0.6488	0.0575	0.0498	0.1000	0.0653	0.0836	0.0373	0.0067
$k+3$	0.9091	0.8946	0.3594	0.0287	0.0211	0.0232	0.0288	0.0421	0.0297	0.0065
$k+4$	0.8397	0.7998	0.1175	0.0267	0.0268	0.0154	0.0119	0.0061	0.0051	0.0173
$k+5$	0.8004	0.7688	0.2070	0.0100	0.0078	0.0109	0.0146	0.0367	0.0262	0.0098

Table 5
Prediction results of 10 bearing testing data sets by using the proposed method.

Data set	31	32	33	34	35	36	37	38	39	40
Actual failure time interval	30	53	16	24	32	28	23	31	19	11
Predicted failure time interval	29.25	50.25	15.88	23.25	29.89	27	22.33	29.78	18.6	11
Predicted failure time interval (determined)	30	51	16	24	30	27	23	30	19	11
Absolute error	0	2	0	0	2	1	0	1	0	0
Accuracy (%)	100	96.23	100	100	93.75	96.43	100	96.77	100	100

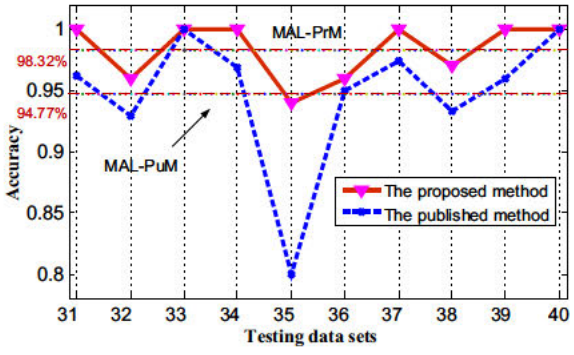

Fig. 8. Accuracy comparison between two methods. MAL-PuM notes 'The mean accuracy line of the published method' and MAL-PrM represents 'The mean accuracy line of the proposed method'.

For further validation of the proposed method, here we compared the predicted results with that obtained in [19] published in the journal of Mechanical Systems and Signal Processing. The mean prediction accuracy obtained by the proposed method is 98.32%, which is greater than 94.77% achieved through the method in [19]. Furthermore, the corresponding testing results of the two methods were demonstrated intuitively in Fig. 8 for a better comparison. The preceding clearly shows that the proposed method has a higher accuracy than that in the existing method.

In addition, the survival probabilities of time intervals were used to predict the machine component health state. The actual high accuracy obtained by methods in this paper and in [7,19] and could be attributed to the time interval representing a relatively long time span in reality (in this paper, one time interval is equal to 1 day). Thus, the accuracy is only 100% if the predicted and actual failure time intervals would fall in the same day. Nevertheless, the proposed method is a promising intelligent prognostics system for machine component health when an appropriate time interval is chosen according to real life situations.

5. Conclusions

To solve the issue that only truncated histories are available, in this study, we conducted further research based on the related published paper. TRIM, which has the ability to highlight the intrinsic health state evolutionary laws within the corresponding truncated histories, was developed. It involves the vital element of state evolution (time) and establishes a state evolutionary manifold space by utilizing both local geometrical structures and global isometric features of a given truncated data set. With the help of FFNN as well as the two defined geometrical metrics (NGD and CGD), a geometrical metric based health prognostics approach for machine component with only truncated histories was developed to maximize the usage of all the useful information within truncated histories. The detailed prognostics process of bearings was conducted to validate the proposed method. Results demonstrate that the proposed method can highlight the intrinsic health state evolutionary laws by TRIM. The more accuracy prognostics results can be consequently achieved based on the cognition of the evolutionary laws.

Acknowledgments

This study was supported by the Fundamental Research Funds for the Central Universities (Grant Nos. YWF 14 KKX 015 and YWF 16 BJ J 18), the National Natural Science Foundation of China (Grant Nos. 61603016 and 51575021), the China Postdoctoral Science Foundation (Grant No. 166482), as well as the Technology Foundation Program of National Defense (Grant No. Z132013B002).

References

[1] A.K.S. Jardine, D. Lin, D. Banjevic, A review on machinery diagnostics and prognostics implementing condition-based maintenance, Mech. Syst. Signal Process. 20 (2006) 1483–1510.
[2] A. Heng, S. Zhang, A.C.C. Tan, J. Mathew, Rotating machinery prognostics: state of the art, challenges and opportunities, Mech. Syst. Signal Process. 23 (2009) 724–739.
[3] J.N. Pan, Reliability prediction of imperfect switching systems subject to multiple stresses, Microelectron. Reliab. 37 (1997) 439–445.
[4] M.E. El-Adll, Predicting future lifetime based on random number of three parameters Weibull distribution, Math. Comput. Simulat. 81 (2011) 1842–1854.
[5] A.K. Schömig, I. Technologies, O. Rose, On the suitability of the Weibull distribution for the approximation of machine failures, in: Proceedings of the Industrial Engineering Research Conference, Portland, OR, 2003.
[6] Z. Tian, A neural network approach for remaining useful life prediction utilizing both failure and suspension data, in: Reliability and Maintainability Symposium (RAMS) 2010 Proceedings - Annual, 2010, pp. 1–6.
[7] S.Y.A. Heng et al, Machine prognosis with full utilization of truncated lifetime data, in: Proceedings of the Second World Congress on Engineering Asset Management, 2007, Harrogate, UK, 2007, pp. 1–10.
[8] C.J. Lu, W.Q. Meeker, Using degradation measures to estimate a time-to-failure distribution, Technometrics 35 (1993) 161–174.
[9] Z. Tian, L. Wong, N. Safaei, A neural network approach for remaining useful life prediction utilizing both failure and suspension histories, Mech. Syst. Signal Process. 24 (2010) 1542–1555.
[10] A. Widodo, B. Yang, Machine health prognostics using survival probability and support vector machine, Exp. Syst. Appl. 38 (2011) 8430–8437.
[11] N. Gebraeel, A. Elwany, J. Pan, Residual life predictions in the absence of prior degradation knowledge, IEEE Trans. Reliab. 58 (2009) 106–117.
[12] X. Fang, R. Zhou, N. Gebraeel, An adaptive functional regression-based prognostic model for applications with missing data, Reliab. Eng. Syst. Saf. 133 (2015) 266–274.
[13] M.J. Kim, V. Makis, Joint optimization of sampling and control of partially observable failing systems, Oper. Res. 61 (2013) 777–790.
[14] L. Bian, N. Gebraeel, Stochastic framework for partially degradation systems with continuous component degradation-rate-interactions, Naval Res. Logist. (NRL) 61 (2014) 286–303.
[15] X. Zhang, L. Xiao, J. Kang, Degradation prediction model based on a neural network with dynamic windows, Sensors 15 (2015) 6996–7015.
[16] R.R. Zhou, N. Serban, N. Gebraeel, H.G. Müller, A functional time warping approach to modeling and monitoring truncated degradation signals, Technometrics 56 (2014) 67–77.
[17] J.B. Tenenbaum, V.D. Silva, J.C. Langford, A global geometric framework for nonlinear dimensionality reduction, Science 5500 (2000) 2319–2323.

[18] H. Qiu, J. Lee, J. Lin, G. Yu, Robust performance degradation assessment methods for enhanced rolling element bearing prognostics, Adv. Eng. Inform. 17 (2003) 127–140.
[19] C. Lu, L. Tao, H. Fan, An intelligent approach to machine component health prognostics by utilizing only truncated histories, Mech. Syst. Signal Process. 42 (2014) 300–313.
[20] K.S. Wang, F.S. Hsu, P.P. Liu, Modeling the bathtub shape hazard rate function in terms of reliability, Reliab. Eng. Syst. Saf. 75 (2002) 397–406.